

(Preprint) AAS 18-246

ENHANCED STATIONKEEPING MANEUVER CONTROL TECHNIQUE FOR DELTA-V COST REDUCTION IN THE KOREA PATHFINDER LUNAR ORBITER

Diane C. Davis,^{*} Jae-ik Park,[†] Sujin Choi,[‡] Ryan Whitley,[§] John Carrico,^{**}
Dong-Young Rew,^{††} and Seok-Weon Choi^{‡‡}

This paper proposes an enhanced control technique for stationkeeping maneuvers to reduce Δv costs for the Korea Pathfinder Lunar Orbiter (KPLO). A scheduled circularization control technique exploits patterns in the evolution of the line of apsides and eccentricity to achieve a significant reduction in stationkeeping Δv costs based on spacecraft requirements. The technique is compared against previous algorithms implemented for maneuver operations of the Lunar Prospector and Lunar Reconnaissance Orbiter (LRO) missions in the USA and KAGUYA in Japan. Through Monte Carlo analysis, the efficacy and robustness of the proposed method are verified, and the technique is shown to meet the operational requirements of KPLO.

INTRODUCTION

The Korea Pathfinder Lunar Orbiter (KPLO) is a lunar exploration spacecraft developed by the Korea Aerospace Research Institute (KARI). Planned for launch late in 2020, KPLO will spend a year in a 100 km circular polar science orbit around the Moon. South Korea's first mission beyond Earth orbit, KPLO's purpose is to implement and verify new space technology, for example, core technology for lunar exploration, scientific research on the lunar environment, and space internet technology.

After launch on a commercial launch vehicle, KPLO will execute a month-long transfer to the Moon that includes 3.5 phasing loops.¹ Lunar orbit insertion will be accomplished by a series of LOI maneuvers that lower the spacecraft into a 100 km circular orbit. A month-long commissioning phase will be followed by at least 11 months of science operations at the Moon. Gravitational perturbations by the lunar gravity field as well as the Earth and Sun will increase orbit eccentricity and eventually lead to impact with the surface of the Moon, so an effective but low-cost stationkeeping scheme is required.

Past missions to circular, polar lunar orbits have effectively implemented orbit maintenance algorithms to maintain spacecraft within eccentricity or altitude requirements. NASA's Lunar Prospector (LP) mission flew in a 100 km circular polar orbit similar to the planned KPLO orbit from January 1998 through July

^{*} Principal Systems Engineer, a.i. solutions, Inc., 2224 Bay Area Blvd, Houston TX 77058.

[†] Senior Researcher, Korea Aerospace Research Institute, 169-84 Gwahak-ro, Yuseong-gu, Daejeon 34133.

[‡] Senior Researcher, Korea Aerospace Research Institute, 169-84 Gwahak-ro, Yuseong-gu, Daejeon 34133.

^{§§} Deputy Systems Integration Manager, Exploration Mission Planning Office, NASA Johnson Space Center, 2101 NASA Parkway, Houston, Texas 77058.

^{**} Chief Technology Officer, Space Exploration Engineering Corp., Baltimore, MD 21202.

^{††} Principal Researcher, Korea Aerospace Research Institute, 169-84 Gwahak-ro, Yuseong-gu, Daejeon 34133.

^{‡‡} Director, Korea Lunar Exploration Program Office, Korea Aerospace Research Institute, 169-84 Gwahak-ro, Yuseong-gu, Daejeon 34133.

1999.^{2,3} Japan's Kaguya mission also orbited in a 100 km circular polar orbit from September 2007 through June 2009.⁴ The Lunar Reconnaissance Orbiter, a NASA mission in orbit since June 2009, maintained a lower 50 km circular polar orbit for 2.5 years before transitioning to a frozen orbit for extended operations.⁵⁻⁸ All three missions maintained circular polar orbits within deadband ranges by implementing a stationkeeping algorithm that controls the evolution of the osculating eccentricity and line of apsides using scheduled burns visible from Earth. The current investigation modifies this algorithm for the KPLO orbit, developing a scheduled circularization control scheme with the goal of decreasing the Δv required for orbit maintenance.

MISSION DESCRIPTION

The KPLO spacecraft will carry six scientific payloads. These include the LUNar Terrain Imager (LUTI), designed to map the surface, seek future landing sites, and identify locations of interest on the lunar surface; as well as the Wide Field Polarimetric Camera (PolCam), which will perform a polarimetric imaging survey of the entire lunar surface in three spectral bands. It will carry the KPLO Gamma Ray Spectrometer (KGRS), designed to map the distribution of various elements and radiation on and beneath the lunar surface; the KPLO Magnetometer (KMAG), which will characterize lunar magnetic anomalies and investigate the origin of lunar crustal magnetism; and the Disruption Tolerant Networking experiment payload (DTNPL). Additionally, a NASA payload will be carried by KPLO, Shadowcam, designed to explore permanently shadowed regions in craters at the poles.

The onboard communication device on KPLO will transmit status reports and scientific data and receive commands in both S- and X- bands. A set of four 30 N thrusters using mono-propellant will control the trajectory of this orbiter, including translunar injection (TLI), lunar orbit insertion (LOI), and station-keeping maneuvers. Attitude will be maintained with 3-axis control through its reaction wheels as well as a set of four 5 N thrusters. Figure 1 shows the KPLO configuration and payloads.

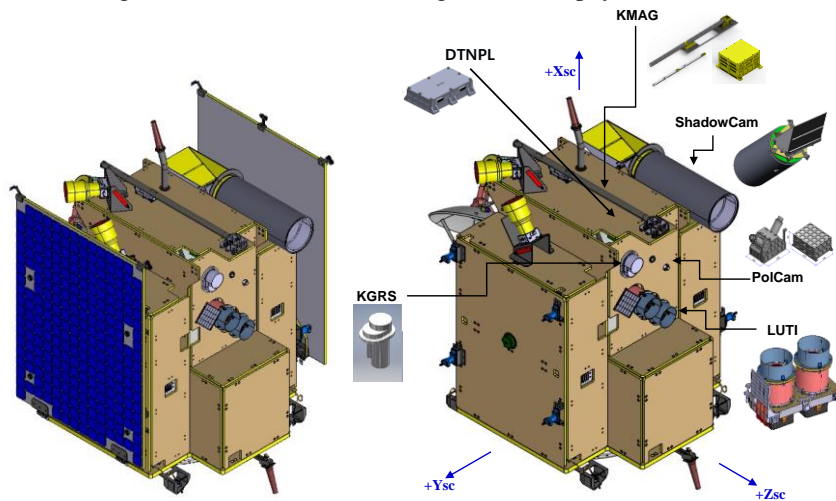


Figure 1. KPLO Configuration and Payloads

The KPLO spacecraft is planned to launch on a Falcon 9 rocket from Cape Canaveral, Florida, as early as December 2020. After launch, the spacecraft will execute a series of three apogee raise maneuvers, approaching the moon after a cruise of approximately a month in three phasing loops. At the Moon, a series of three lunar orbit insertion maneuvers will lower the spacecraft into its circular science orbit. The transfer trajectory appears in Figure 2; further details appear in Choi et al.¹

The KPLO science orbit is nominally at an altitude of 100 km. Excursions from the nominal are desired to remain less than 30 km, though occasional small violations of the ± 30 km deadband for short durations are deemed acceptable. The preferred inclination is precisely 90° to provide visibility of shadowed craters at the poles. Gravitational perturbations cause the inclination to drift over time, with the magnitude and direction of the drift depending on insertion epoch. Insertion inclination is adjusted to maximize duration of the science operations at 90° inclination. The stationkeeping Δv budget is 75 m/s for the year-long mission.

In the current analysis, a 75x75 a 75x75 GRAIL0660B lunar gravitational field model is used, and third body effects for the Sun and Earth are considered. Solar radiation pressure (SRP) is also considered in portions of the study.

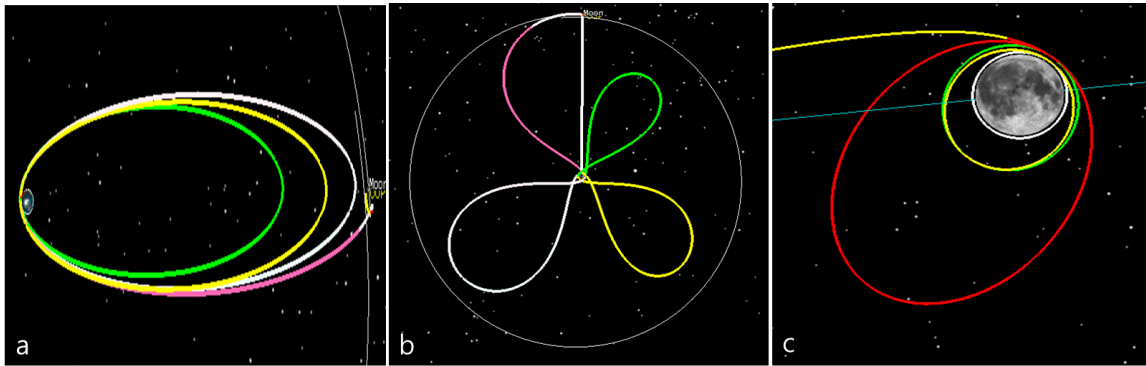


Figure 2. Transfer orbit from launch to science orbit insertion. Earth-centered inertial view (a), Earth-Moon Rotating View (b) and Moon centered inertial view (c).

EVOLUTION OF ECCENTRICITY AND LINE OF APSIDES

Without orbit maintenance, a spacecraft inserted into a circular polar orbit with an altitude of 100 km will impact the lunar surface after about 200 days. Gravitational perturbations from the lunar gravity field, as well as third body effects from the Earth and Sun, cause the eccentricity of the orbit to generally increase over time until impact occurs. The evolution of the orbital elements is not random, however. In particular, the evolution of the line of apsides and eccentricity (e) of a polar orbit at the Moon follows distinct patterns,²⁻⁸ and these patterns are employed to design effective algorithms for orbit control. A sample pattern appears in a polar plot in Figure 3a, with eccentricity along the radius and argument of perilune (ω) as the angular value. With an eccentricity at orbit insertion of $e = 0.018$ and argument of perilune $\omega = 217^\circ$, the orbit starts just outside the deadband at an altitude of 133 km at the marked insertion state. The eccentricity decreases in a repeating e - ω pattern, moving clockwise and to the right in Figure 3a, until the orbit is nearly circular. The eccentricity then begins to grow again, continuing to evolve in the same e - ω pattern, until the orbit departs the ± 30 km deadband and eventually impacts the lunar surface after 236 days. The altitude over time of the same propagation appears in Figure 3b, with ± 30 km deadbands marked in green. The same behavior (decreasing, then increasing eccentricity) is seen in the altitude pattern, until the spacecraft impacts at an altitude of 0 km.

Instead of allowing the orbit to freely evolve until impact, orbit maintenance maneuvers (OMM) are implemented to exploit the patterns in eccentricity and argument of perilune to control the spacecraft and keep it in orbit and within given altitude deadbands throughout the operational period. A pair of maneuvers allow the spacecraft to jump from one location on the e - ω polar plot to another. In general, the longer the distance along the plot the spacecraft must travel, the more costly the maneuver.

Patterns of evolution in the e - ω polar plot have been exploited in the past to successfully maintain LP,²⁻³ Kaguya,⁴ and LRO.⁵⁻⁸ These three missions all employed a line-of-apsides control method that targets a specific e - ω pair. The OMMs occur at regular intervals, as the patterns in the e - ω evolution repeat on a monthly basis. LRO flew at an altitude of 50 km with a ± 20 km deadband during its primary science operations, and it executed a pair of maneuvers once per lunar month, about every 27.4 days. Maneuvers were scheduled when the right ascension of the ascending node (RAAN) of the orbit was approximately 270° . This constraint ensured that both maneuvers in the pair were visible from Earth. A sample of the e - ω evolution followed by a trajectory similar to the one flown by LRO appears in Figure 4a. Note the repeating pattern. Insertion occurs at the blue point to the left of the plot, with initial conditions $a = 1787$ km, $e = 0.0075$, $\omega = 160^\circ$, $i = 90^\circ$, and RAAN = 270° . The trajectory evolves over time in the direction of the blue arrows. The first burn in the OMM pair occurs at the red point on the righthand side; the eccentricity and RAAN have approximately returned to their original values, but the argument of perilune is about 20° . The first burn in the pair, occurring at a true anomaly of about 150° , targets an intermediate orbit with an argu-

ment of perilune of about 90° at apolune on a transfer arc. The second burn (also in red) then targets back to the original values of a , e , and ω at the next perilune. To remain within the ± 20 km deadband, a monthly maneuver set is necessary. Figure 4a represents 13 maneuver pairs, a propagation time of 380 days, and a total maneuver cost of 141 m/s. The average of 10.8 m/s per maneuver pair is in line with the observed average of 11.1 m/s for each of the first 6 maneuver pairs of LRO science operations, as reported by Mesarch et al.⁵

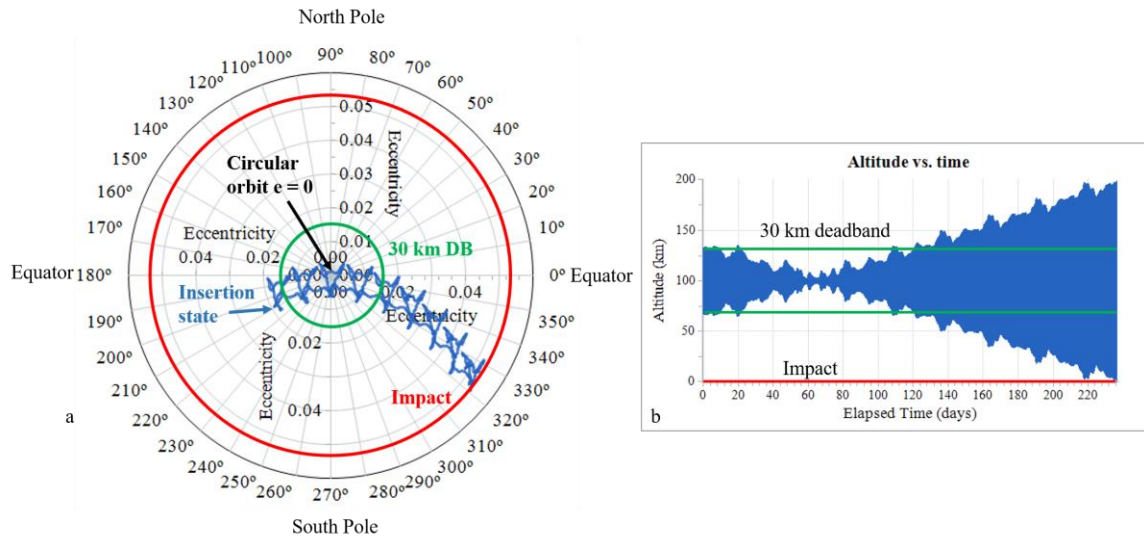


Figure 3. Evolution of argument of perilune and eccentricity over time (blue) for an uncontrolled spacecraft in an e - ω polar plot (a). Approximate eccentricity corresponding to a 30 km deadband marked in green, impact in red. Altitude vs. time for the same insertion conditions (b).

LP and Kaguya each flew in a higher 100 km orbit, similar to the one planned for KPLO. With a ± 20 km deadband requirement, LP performed maneuvers about every 55 days using a line-of-apsides control scheme. Kaguya, with a ± 30 km requirement,⁴ implemented a similar scheme. An e - ω history for a trajectory similar to LP's selected orbit appears in Figure 4b. The insertion state, corresponding to $a = 1837$ km, $e = 0.0095$, $\omega = 160^\circ$, and $RAAN = 270^\circ$ is marked by a blue point at the left. After the trajectory evolves over about 54.6 days, the $RAAN$ and eccentricity return to their starting values and the argument of perilune has a value of about 20° . As before, a pair of OMMs targets first to $\omega = 90^\circ$ at apolune on a transfer arc, and then back to the starting conditions in a , e and ω . With the higher 100 km nominal altitude, a maneuver pair is executed every two months. Figure 4b represents 6 maneuver pairs over 382 days for a total Δv of 83.7 m/s, or an average of 14 m/s per OMM pair. This cost corresponds to the average maneuver pair cost of 13.2 m/s observed during the Kaguya mission as reported by Matsumoto et al.⁴ Unsurprisingly, maintaining the higher 100 km orbit within a 20 km deadband has a lower annual cost than maintaining the 50 km orbit within 20 km of its nominal altitude.

Kaguya flew in a 100 km polar orbit with a larger altitude deadband requirement of ± 30 km. The larger deadband allows a longer time span between maneuver pairs, if desired. Consider the e - ω plot in Figure 4c. In this example, the spacecraft is inserted with $a = 1837$ km, $e = 0.0135$, $\omega = 170^\circ$, and $RAAN = 270^\circ$. After three lunar months, or about 82 days, the orbit returns to the original insertion values of eccentricity and $RAAN$, and the argument of perilune has a value of about 15° . A pair of maneuvers again targets to $\omega = 90^\circ$ along a transfer arc, and finally back to insertion values of a , e , and ω . Only 4 maneuver pairs are executed during the 382-day propagation, but each OMM pair is larger, with an average value of 21.8 m/s. The maneuver pair must move the orbit farther across the e - ω plot, corresponding to the higher cost of each OMM pair. The total annual Δv in this case is 87.2 m/s. Though the deadbands are higher than in the example in Figure 4b, the cost is not lower; in fact, the annual Δv is nearly 4 m/s higher.

It is possible to increase the deadbands to ± 40 km by inserting with a higher eccentricity farther left on the polar plot and allowing the e - ω pattern to evolve for four months. An example appears in Figure 4d, with insertion values $a = 1837$ km, $e = 0.017$, $\omega = 180^\circ$, and $RAAN = 270^\circ$. Executing a burn pair every 4

months results in still larger distances to cross along the e - ω plot, thus increasing the cost of each OMM pair to 30.5 m/s on average. The total stationkeeping cost of the three OMM pairs grows to 91.5 m/s. The current investigation explores a method to decrease the distance traveled along the e - ω plot, and hence the total annual stationkeeping Δv .

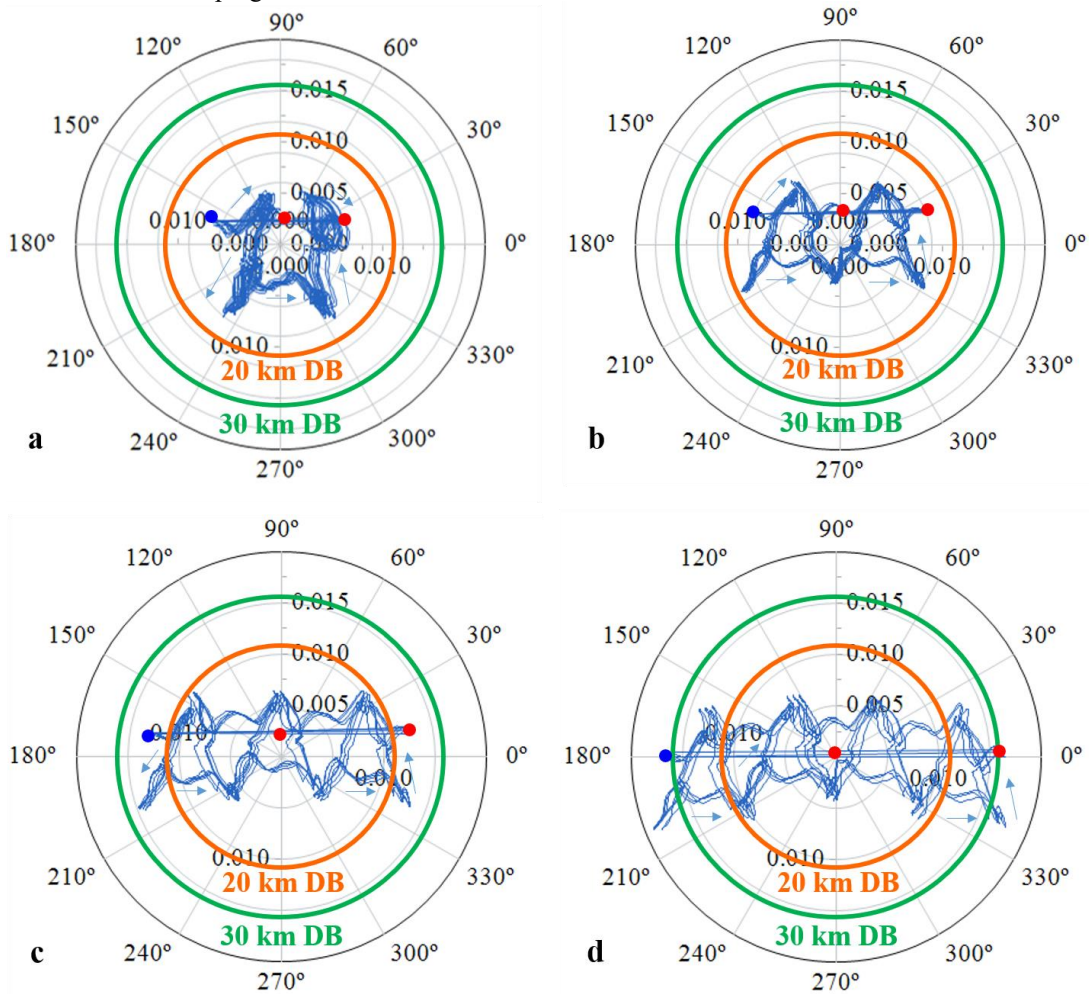


Figure 4. Evolution of argument of perilune and eccentricity over time for circular polar lunar orbits with line-of-apsides control. 50 km \pm 20 km (a), 100 km \pm 20 km (b), 100 km \pm 30 km (c), and 100 km \pm 40 km orbits (d).

SCHEDULED CIRCULARIZATION CONTROL

The polar plots in Figure 4 demonstrate the application of line-of-apsides control to effectively maintain circular lunar orbits by exploiting repeating patterns in eccentricity and argument of perilune. As the deadbands grow in Figures 4b, 4c, and 4d, the distances between the red points (representing OMMs) also increase. That is, the larger the deadband, the longer the distance within the e - ω plot that each OMM pair must traverse. The OMM magnitude increases as well. To reduce the total stationkeeping Δv , the line-of-apsides control algorithm is modified to reduce the distance along the e - ω plot traversed after each OMM pair.

The insertion state is selected such that the trajectory evolution begins at the far left of the e - ω plot. The orbit is allowed to evolve for three or more months before the first OMM pair is executed. Instead of targeting back to the insertion values of eccentricity and argument of perilune, however, a Hohman transfer is executed to circularize the orbit. This alternate OMM pair moves the orbit to the center of the e - ω plot, where a new pattern is initiated. The trajectory is allowed to evolve for two months between each subse-

quent OMM pair, each of which re-circularizes the orbit. As in the line-of-apsides control scheme, the burns are executed at RAAN = 270°, ensuring both maneuvers in the pair are visible from Earth. Two samples are explored, one with a starting RAAN = 50°, one with an insertion RAAN = 230°. These two orbit options represent favorable insertion conditions from the Earth-to-Moon transfer.¹ Initial conditions for the two orbits appear in Table 1.

Table 1. KPLO science orbit options: insertion conditions

| | RAAN = 50° | RAAN = 230° |
|------------------|------------|-------------|
| Epoch | 1-Jan-2021 | 1-Jan-2021 |
| Semi-major axis | 1837 km | 1837 km |
| eccentricity | 0.018 | 0.012 |
| inclination | 89.45° | 90.28° |
| arg. Of perilune | 217° | 190° |
| RAAN | 50° | 230° |
| True Anomaly | 264° | 2° |

The first orbit example appears in Figure 5. Orbit insertion is marked by a blue point on the lower left of the e - ω plot in Figure 5a. The orbit is allowed to drift through e - ω space for 3.5 maneuver-free months at the start of the mission without violating deadbands. The first set of OMMs is then executed when RAAN reaches a value of 270°, marked by red points in Figure 4a. This OMM pair targets a 100 km circular orbit. Because the insertion state is carefully selected such that the OMM location in e - ω space is near $\omega = 0$, the OMM traverses a very short distance within the e - ω plot, and the corresponding Δv magnitude is just 7.1 m/s. The spacecraft is then propagated for 2 lunar months, and a second burn pair (marked in orange) targets back to altitude = 100 km and eccentricity = 0. This 2-month pattern is repeated, with a Hohman transfer circularizing the orbit at each OM opportunity. The subsequent four burn pairs average 12.7 m/s each, for a total annual stationkeeping cost of 58.0 m/s. The cumulative Δv magnitude over time appears in Figure 5b. This cost represents a savings of 25.7 m/s over line-of-apsides control for the first year in the 100 km circular polar orbit. Since the algorithm circularizes the orbit at regular intervals, it is denoted scheduled circularization control (SCC).

The cost savings achieved using SCC requires a tradeoff. The line-of-apsides control method maintains the spacecraft within ± 20 km of the nominal 100 km altitude, and as demonstrated, increasing the deadbands to 30 km or even 40 km does not decrease the cost. In the SCC method, however, cost savings are achieved by relaxing the deadband. The spacecraft altitude history appears in Figure 5c. Green lines mark ± 30 km deadbands, and the OMM pairs are marked by red and orange points. Every 2 months, the orbit violates the 30 km limit for about 3 days. The maximum and minimum altitudes reached in this example are 134 km and 65 km respectively, each occurring shortly after insertion during the first month of operations. The average altitude over the year is 100 km, and the altitude returns to 100 km at each OMM burn as the eccentricity is targeted to zero.

The inclination at orbit insertion affects the OM cost. The starting inclination in the RAAN = 50° example, $i = 89.45^\circ$, is selected to ensure that the spacecraft achieves 90° inclination throughout the first year of operations, and to continue the 90° inclination passages through a possible extended mission. The secular trend in inclination for the RAAN = 50° orbit with a Jan 1, 2021 insertion is positive, so the starting inclination is selected below the nominal 90°. The inclination history appears in Figure 5d.

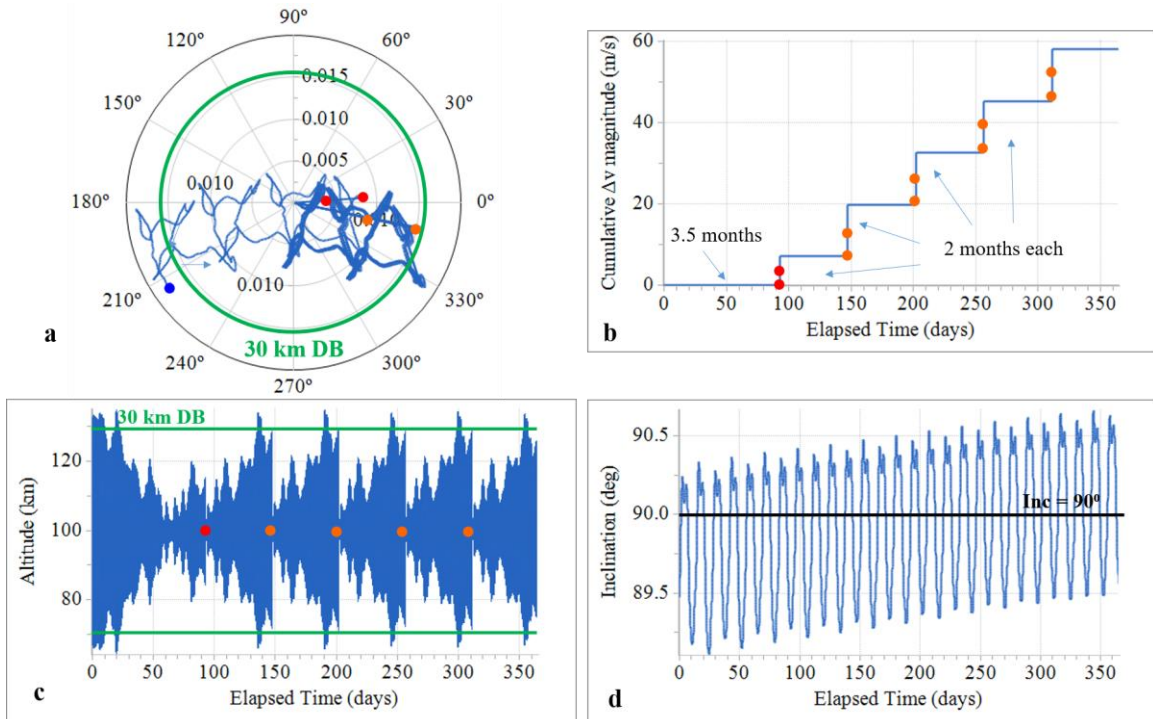


Figure 5. SCC algorithm controls the RAAN = 50° orbit for one year. Polar e - ω plot (a). Cumulative Δv history (b). Altitude history (c). Inclination history (d).

A second example represents an insertion on the other side of the Moon. With a starting RAAN = 230°, the initial value of ω is selected such that the argument of perilune evolves through the southern hemisphere, as in Figure 6a. After nearly three lunar months, the orbit reaches RAAN = 270° and the first OMM pair is executed. At this point, marked in red in Figure 6a, the eccentricity is relatively low and ω is near zero. As a result, to reach the center of the e - ω polar plot, the OMM pair traverses only a short distance in e - ω space, and the required Δv to circularize the orbit is only 6.0 m/s. As depicted in Figure 6b, the subsequent maneuvers occur every 2 lunar months, always when RAAN = 270° for visibility from Earth. The next four maneuver pairs average 12.4 m/s each, and the total stationkeeping cost for the first year is 55.7 m/s.

The altitude profile appearing in Figure 6c shows, again, small excursions beyond 130 km and 70 km altitude for about 3 days every two months. The starting inclination, depicted in Figure 6d, is selected to be greater than 90° to compensate for the negative secular trend in inclination for an insertion date of Jan 1, 2021.

The RAAN = 230° sample orbit is extended for two years to simulate an extended mission and to assess the cost savings vs. line of apsides control over a longer time frame. In a two-year simulation, the first OMM pair occurs after 3 lunar months, and the subsequent 11 OMM pairs occur every 2 lunar months. The tight pattern in e - ω space is maintained, and the total Δv for two years of stationkeeping is 141.6 m/s. In comparison, a 2-year propagation of the orbit featured in Figure 4b using line-of-apsides control with maneuvers every 2 lunar months costs 180.3 m/s. The two altitude profiles and e - ω polar plots appear in Figure 7. The inclination of both orbits passes through 90° throughout the entire two-year period. Over the two-year mission, the SCC algorithm saves about 40 m/s over line-of-apsides control for a 100 km circular polar orbit if a wider deadband is acceptable.

Both the RAAN = 50° sample orbit and the RAAN = 230° sample orbit are integrated with the Earth to Moon transfer trajectory optimization (see Figure 0) to ensure that the insertion conditions are compatible with the transfer trajectory. In both cases, insertion into the favorable orbits is achieved with negligible changes to the total transfer cost as compared to insertion into a circular polar orbit with RAAN and ω left free to vary. That is, specifying particular insertion conditions to ensure favorable stationkeeping costs does not adversely affect the total cost of the integrated mission.

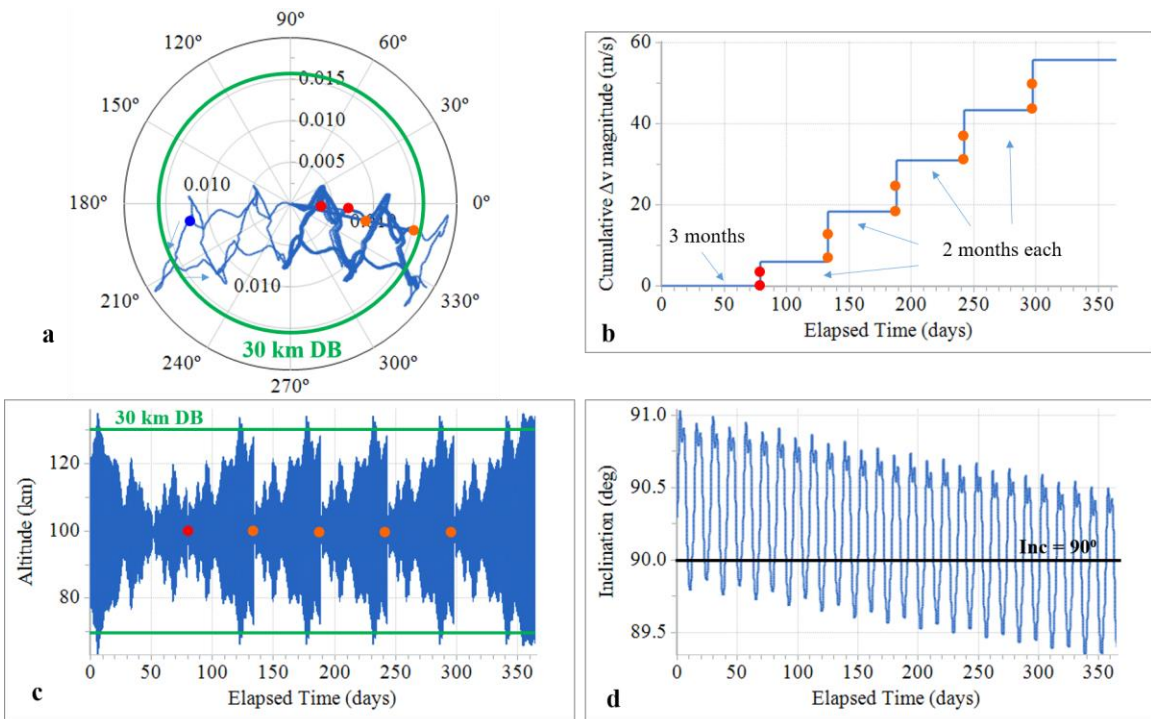


Figure 6. SCC algorithm controls the RAAN = 230° orbit for one year. Polar $e-\omega$ plot (a). Cumulative Δv history (b). Altitude history (c). Inclination history (d).

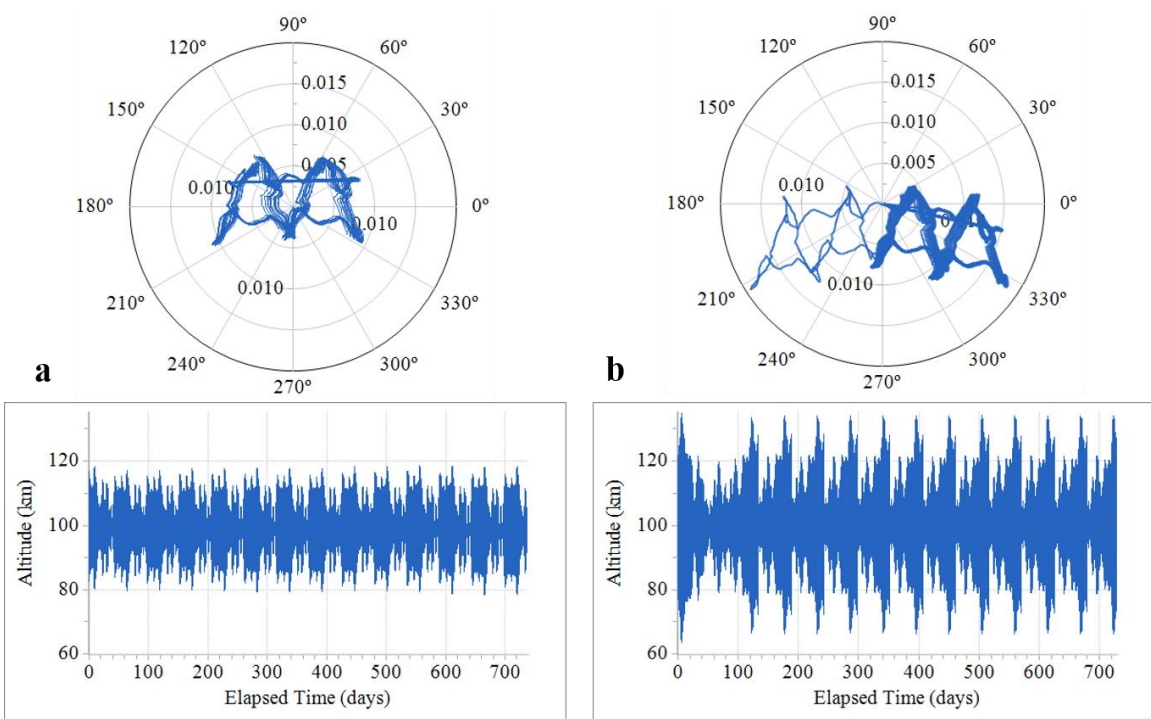


Figure 7. Altitude and $e-\omega$ profiles for two-year propagations of a 100 km circular polar orbit using line-of-apsides control for a cost of 180.3 m/s (a) and SCC for a cost of 141.6 m/s (b).

VARYING INSERTION DATES

For a given set of initial conditions at the Moon, the evolution of the osculating elements over time, as well as annual station keeping costs, vary depending on insertion date. The two example orbits in Table 1 are considered for insertion epochs daily between January and December 2021. Results for the RAAN = 50° case appear in Figure 8. For every day in 2021, a spacecraft is inserted into orbit at Moon with the orbital elements listed in Table 1. Each insertion state is then propagated forward for a year to assess annual stationkeeping costs, minimum and maximum altitudes, and the range of inclination values over the year.

Annual stationkeeping costs as a function of insertion date appear in Figure 8a. Costs are characterized by a short period repeating every month as well as a negative secular trend, but variations are small. The maximum cost of 58 m/s occurs with insertion at the beginning of January, and the minimum annual cost of 55.6 m/s is achieved with orbit insertion in mid-December.

Variations in the minimum and maximum altitudes experienced by the spacecraft are also small; results appear in Figures 8b and d. For insertion dates at the beginning of the year, the altitudes tend to remain higher with larger values for both maximum and minimum altitude during a one-year mission. If the spacecraft inserts later in the year, the minimum altitude it experiences will likely be lower, as will the maximum altitude during the mission. Again, a four-week period is apparent in the data.

Variations in minimum and maximum inclination values over a year-long mission appear in Figure 8c for insertion dates throughout 2021. For example, a spacecraft inserting on Jan 1, 2021 experiences a minimum inclination of 89.4° and a maximum inclination of 91° during its year-long mission, while the same insertion state on Jan 7, 2021 corresponds to a minimum inclination of 88.7° and a maximum inclination of 90.5° during a year's science operations. The pattern in inclination trends repeats every lunar month without a secular trend. That is, for a given set of insertion elements, the insertion date determines whether the inclination increases during the year-long mission or if the inclination decreases through the year. By customizing insertion inclination based on insertion date, $i = 90^\circ$ passages are maintained throughout one year (or longer) science operations phases regardless of insertion date. Preferred values of inclination at insertion are explored further in the following section.

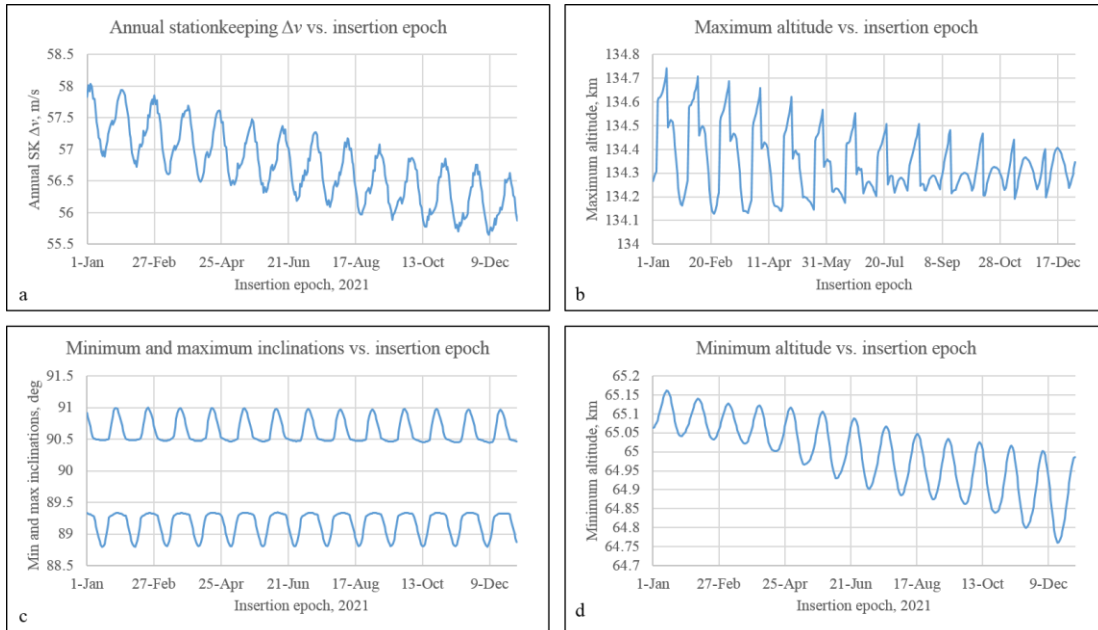


Figure 8. Variations in cost (a), maximum and minimum altitudes (b,d), and maximum and minimum inclinations (c) for year-long science operations as a function of insertion epoch in 2021 for RAAN = 50° insertion conditions from Table 1

Similarly, variations in behavior of cost, altitude, and inclination based on insertion date for the RAAN = 230° set of insertion elements from Table 1 appear in Figure 9. Again, the maximum costs are associated

with insertion dates at the beginning of the year, with a four-week pattern throughout the year. Altitudes also vary with a monthly period, with the largest maximum altitudes corresponding to the largest minimum altitudes, so that the total altitude range (minimum to maximum) for any given insertion epoch does not vary widely. The inclination variations again follow a four-week period without a secular trend, but where the RAAN = 50° orbit starts the year with a positive slope in inclination, the RAAN = 230° orbit has a negative slope in inclination with a Jan 1, 2021 insertion date. That is, the two sets of insertion conditions are out of phase in inclination trends.

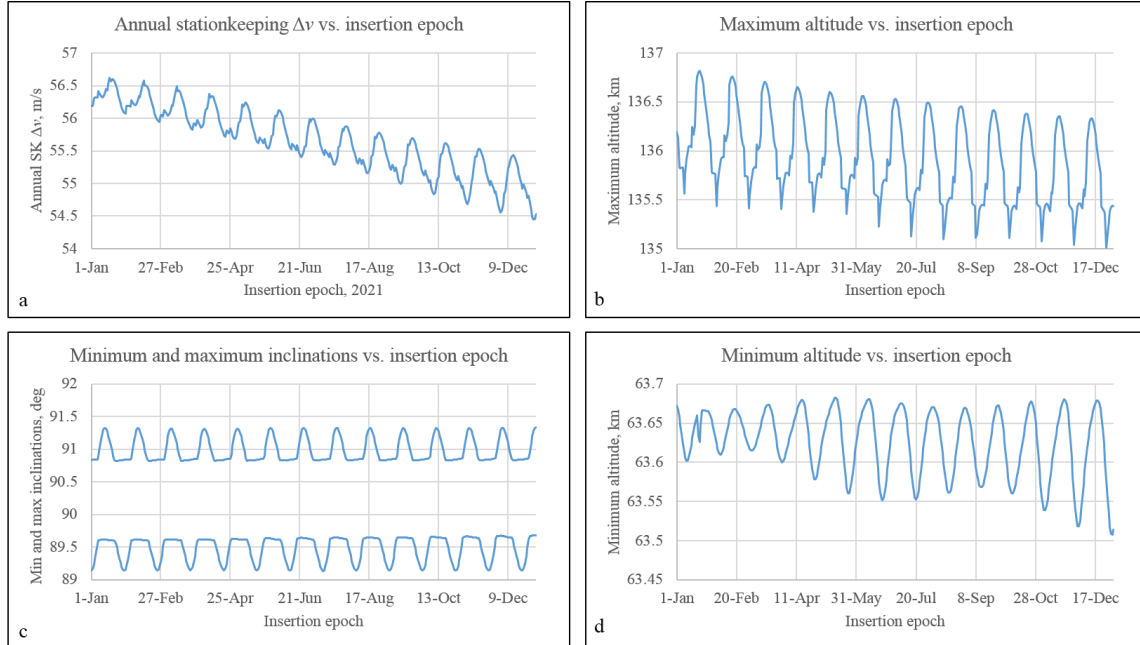


Figure 9. Variations in cost (a), altitude (b), and inclination (c) for year-long science operations as a function of insertion epoch in 2021 for RAAN = 230° insertion conditions from Table 1

Inclination Trends

The trends in inclination are significant due to the requirement to pass through $i = 90^\circ$ during science operations. With no secular trend, the patterns in inclination evolution repeat each lunar month. A zoomed view of the first month of the plot from Figure 8c appears in Figure 10a. This view displays the inclination range over a 1-year science mission as a function of insertion date for the RAAN = 50° sample orbit from Table 1. Insertion occurs each day during the month of January 2021. For example, consider the first data-point corresponding to insertion on Jan 1, 2021. The inclination evolution appears in Figure 10b. Note the positive secular trend as inclination evolves over the year; the starting inclination is thus selected to be lower than 90° to enable polar passes throughout the year of operations and into a potential extended mission. The inclination at insertion is 89.45° , and the resulting science orbit is propagated for a year with SCC orbit maintenance. Over the course of a year propagation, osculating inclination ranges from a minimum of 89.1° at the start of science operations to a maximum of 90.7° at the end of the year's operations. A second sample orbit commences on Jan 7, 2021, with initial orbital elements listed in Table 1. This initial state yields an orbit with no significant secular trend in inclination, as in Figure 10c. The inclination of this science orbit remains in a fixed range for extended propagation times. The starting inclination is thus increased to 89.75° to center the inclination pattern on 90° . A third sample appears in Figure 10d. An insertion date of Jan 15, 2021 yields a decreasing trend in inclination. A higher starting inclination is thus desirable; with $i_0 = 90.2^\circ$, the spacecraft makes polar passes throughout the year and is positioned for an extended mission. In summary, initial inclination values for the RAAN = 50° sample orbit range from about 89.45° to about 90.2° when accounting for the secular trends. Adjusting the value of starting inclination based on insertion epoch allows for polar passages throughout the year to ensure favorable conditions for science operations.

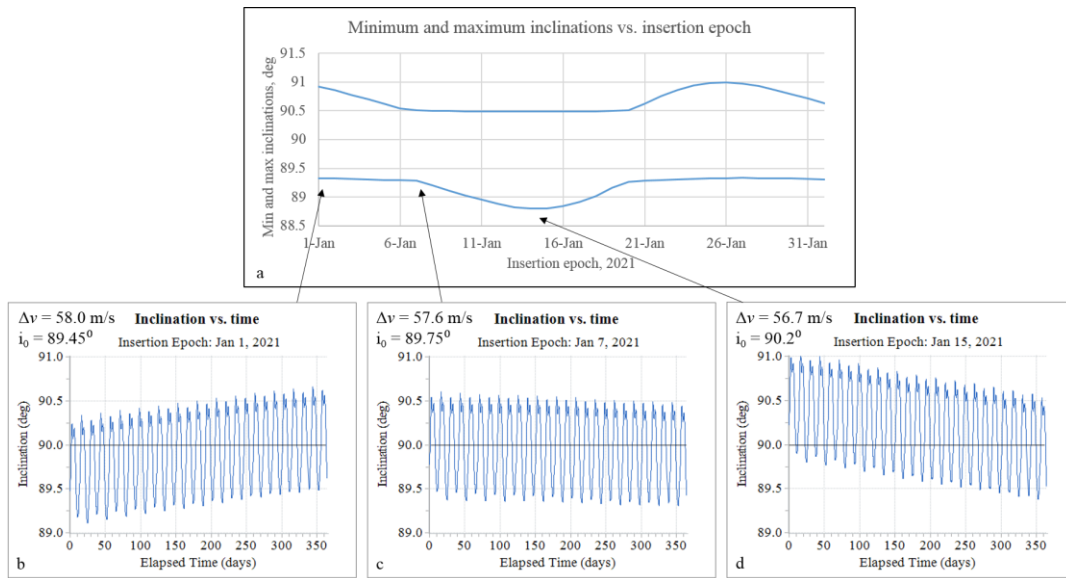


Figure 10. Inclination range over a one-year science mission vs. insertion epoch for January 2021 insertion dates (a). Insertion inclination selected for 90° science operations for insertion on Jan 1, 2021 (b), Jan 7, 2021 (c), Jan 25, 2021 (d). RAAN = 50° sample orbit.

Similar patterns exist in the inclination trends for the RAAN = 230° sample orbit. Inclination ranges for insertion dates in January 2021 appear in Figure 11a. In contrast to the previous example however, osculating inclination decreases over the course of the year for an orbit with insertion date of Jan 1, 2021. To account for the negative slope, the starting value of inclination is selected to be 90.28°. This initial inclination leads to coverage of $i = 90^\circ$ throughout the year of science operations and into a potential second year, as in Figure 11b. Insertion a week later on Jan 7, 2021 results in a near-constant pattern in the osculating inclination. A starting value $i_0 = 89.85^\circ$ thus maintains inclination covering 90° throughout the mission, as demonstrated in Figure 11c. Finally, an insertion epoch of Jan 15, 2021 corresponds to a positive slope in inclination during science operations, and an initial inclination of 89.5° is selected to achieve the desired polar orbit throughout the year, shown in Figure 11d.

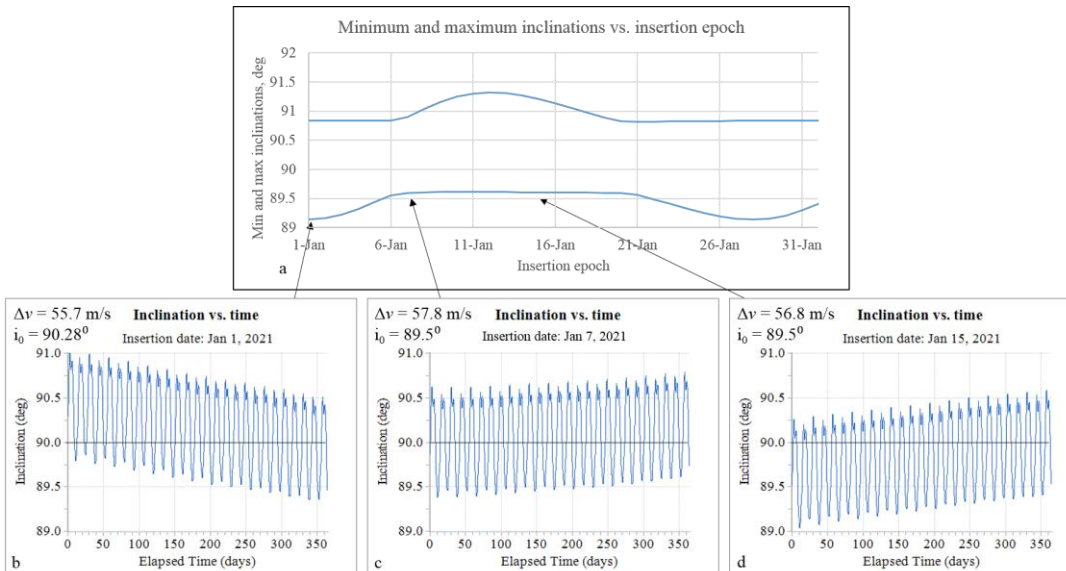


Figure 11. Inclination range over a one-year science mission vs. insertion epoch for January 2021 insertion dates (a). Insertion inclination selected for 90° science operations for insertion on Jan 1, 2021 (b), Jan 7 2021 (c), Jan 25, 2021 (d). RAAN = 230° sample orbit.

Aligning Solar β Angle with Lunar Solstice

For optimal lighting in certain shadowed polar craters, it is desired for the science orbit to reach a solar β angle equal to zero during the lunar solstice. The solar β angle is defined as the angle between the spacecraft's orbital plane and the Moon-Sun vector. Solar $\beta = 0^\circ$ when the orbit is aligned with the Sun and passes through noon and midnight as in Figure 12a, and $\beta = 90^\circ$ when the orbital plane is normal to the Moon-Sun vector, placing the orbit over twilight as in Figure 12b. The value of RAAN at insertion determines the starting value of solar β angle; after insertion, the angle evolves slowly through the year, reaching a value of 0° every 6 months. For a given RAAN value, two launch opportunities per month align $\beta = 0^\circ$ with a solstice; the two solstices occur on March 16, 2021 and August 28, 2021. The insertion epochs each month that lead to the desired conjunction of solstice with $\beta = 0^\circ$ also correspond to the maximum inclination variations.

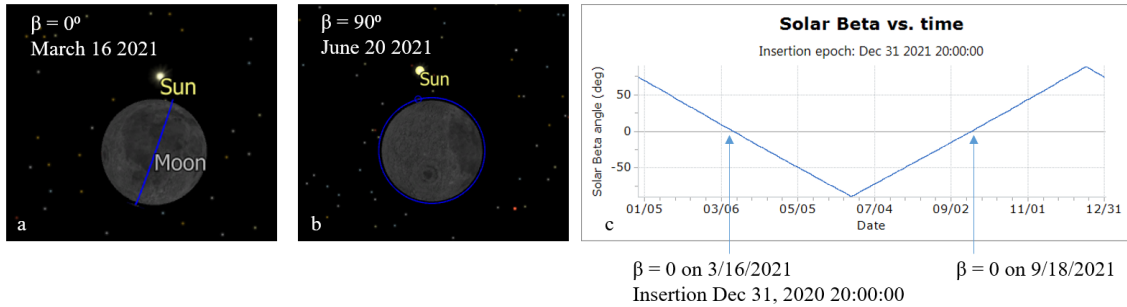


Figure 12. The orbital plane is aligned with the Moon-Sun vector when $\beta = 0^\circ$ (a) and is perpendicular to the Moon-Sun vector when $\beta = 90^\circ$ (b). Insertion on Dec 31, 2020 at 20:00 aligns $\beta = 0^\circ$ with the solstice.

MONTE CARLO ANALYSIS

The stationkeeping costs and trends discussed thus far assume an ideal spacecraft. In reality, errors in navigation and maneuver execution, as well as perturbations due to solar radiation pressure and momentum desaturations, lead to variations in the cost. In the current analysis, a Monte Carlo simulation is performed to explore the robustness of the SCC algorithm and to compare costs with other methods of orbit maintenance. The following errors are considered:

- Insertion error: 200 m position, 2 cm/s velocity, spherical 3σ
- Navigation error: 200 m position, 2 cm/s velocity, spherical 3σ
- Maneuver execution error: 5% magnitude, 5% direction, 3σ
- Solar radiation pressure: 5% area, 10% coefficient of reflectivity, 1σ
- Momentum wheel desaturations, 1 per day, 1 cm/s, 1σ (Included in selected runs)

The purpose of the analysis is to assess the reliability or consistency of the SCC algorithm in a realistic scenario. That is, to assess whether the low cost and the repeatable patterns in the e - ω evolution remain in the presence of spacecraft and navigation errors, and how the costs and reliability compare to other algorithms. First, a simulation is run to assess costs for the SCC algorithm for the RAAN = 50° and RAAN = 230° sample orbits from Table 1. The analysis includes 100 Monte Carlo trials, each propagated for a year, with a Jan 1, 2021 insertion date. The results appear in Table 2. The error-free values also appear in the table. The difference between the minimum cost and the maximum cost for the year-long simulation is less than 2 m/s and differs by less than 1.5 m/s as compared to the case without errors. That is, the SCC algorithm yields a consistent cost even in the presence navigation and spacecraft errors. The minimum and maximum altitudes experienced by the spacecraft vary slightly, by up to 1 km, as compared to the nominal case without errors. The pattern in the e - ω polar plot is maintained in each of the Monte Carlo trials.

Table 2. Annual stationkeeping costs and altitude ranges from a Monte Carlo simulation

| case | Nominal, no errors | | | Monte Carlo Analysis | | | | | |
|-------------|-------------------------|----------------|-----|----------------------|-------------------------|------|------|----------------|-----|
| | Annual Δv (m/s) | Altitudes (km) | | trials | Annual Δv (m/s) | | | Altitudes (km) | |
| | | min | max | | min | mean | max | min | max |
| RAAN = 50° | 58.0 | 65 | 134 | 200 | 57.6 | 58.5 | 59.4 | 64 | 135 |
| RAAN = 230° | 55.7 | 63 | 136 | 200 | 55.8 | 56.5 | 57.6 | 63 | 136 |

The analysis is repeated for four potential stationkeeping algorithms to assess cost and consistency of each. The initial spacecraft state is adjusted separately for each algorithm; different starting elements are more suitable for each. The first two methods explored are the SCC algorithm and the line-of-apsides control algorithm discussed previously. Simulations that include 50 Monte Carlo trials each propagated for a year are run. Results appear in the first two rows of Table 3. Both algorithms provide consistent results that do not vary significantly in the presence of errors. The line-of-apsides control algorithm yields a tighter deadband, with no excursions beyond ± 20 km. The SCC algorithm provides a lower cost at the expense of larger deadbands. Note that desaturations are only considered in the SCC analysis.

The second two algorithms are simple deadband control algorithms. Neither takes advantage of the repeatable patterns in e - ω evolution; a maneuver is simply executed when a deadband is violated. The first deadband control algorithm performs a Hohmann transfer to circularize the orbit to 100 km altitude each time the ± 30 km deadband is reached. The second method is a one-sided control method; a single burn is executed to correct only the deadband that is violated, either raising perilune to 100 km or lowering apolune to 100 km. A major disadvantage of the simple deadband control algorithms is that the maneuvers are not scheduled in advance: they are unpredictable and unlikely to occur at RAAN = 90° or RAAN = 270°, and thus are not necessarily visible from Earth. In addition, without following the repeatable e - ω pattern, the number of maneuvers performed during the year of science operations, along with the associated cost, varies widely as the characteristics of each trial are affected by navigation and spacecraft errors. In both cases, the no-errors cost is about the same as the minimum cost in the Monte Carlo run. However, the number of maneuvers and the maximum cost are significantly higher; in particular, the deadband control scheme that circularizes the orbit at each deadband violation (row 3 in Table 3) has a maximum cost more than 25 m/s higher than the minimum. The lack of predictability in maneuver cost and frequency associated with the deadband control algorithms make them less favorable for operations.

Table 3. Annual stationkeeping costs and altitude ranges from a Monte Carlo simulation for various stationkeeping algorithms. Desaturation errors only considered for SCC.

| Algorithm | Nominal, no errors | | | | Monte Carlo Analysis | | | | |
|------------------------|-------------------------|----------------|-----|-----------------|-------------------------|------|------|----------------|-----|
| | Annual Δv (m/s) | Altitudes (km) | | maneuver events | Annual Δv (m/s) | | | Altitudes (km) | |
| | | min | max | | min | mean | max | min | max |
| Line of Apsides | 83.7 | 78 | 120 | 6 | 82.0 | 84.1 | 85.8 | 89 | 118 |
| Deadband (circularize) | 80.7 | 70 | 130 | 5 | 68.8 | 80.4 | 94.4 | 70 | 130 |
| Deadband (one-sided) | 79.2 | 70 | 130 | 11 | 77.4 | 79.6 | 91.7 | 70 | 130 |
| SCC | 55.7 | 63 | 136 | 5 | 55.8 | 56.5 | 57.6 | 63 | 136 |

UNCONTROLLED SPACECRAFT DISPOSAL

The current baseline propellant budget does not include an allocation for controlled disposal of the KPLO spacecraft. Instead, the spacecraft is planned to impact the surface of the Moon naturally after science operations cease. Analysis is run to determine potential impact sites and to assess the likelihood of interfering with historical lunar landing sites.

The starting conditions for the disposal analysis assume that KPLO has just completed its final stationkeeping maneuver pair to circularize the orbit to 100 km altitude after a year of science operations. The initial altitude is thus assumed to be 100 km, with a zero eccentricity. The initial values of RAAN and argument of perilune are varied from 0 to 360° in 30° steps. Initial inclination ranges from 88° to 92° in 0.5° steps, since the original orbit insertion conditions (orbital elements and epoch) determine the final value of inclination. The epoch for the final circularization maneuver (and thus the initial epoch for the disposal analysis) is set at Jan 1, 2022. Each starting point is propagated until it impacts the surface of the Moon, without considering navigation, SRP, or maneuver execution errors; orbit divergence is due to the lunar

gravity field and Sun and Earth third-body effects only. Resulting impact points are plotted along with American and Russian historical landing sites on a lunar map in Figure 13.

The predictable evolution of argument of perilune and eccentricity explain the clustering of impact points in the southern hemisphere. Recall the pattern appearing in the $e-\omega$ polar plot in Figure 3a as a spacecraft in a 100 km polar orbit is propagated to impact. At an eccentricity corresponding to a zero altitude, the argument of perilune is approximately 320° . In a polar orbit, this value of ω corresponds to a latitude of about -40° . Each of the starting conditions considered in the impact analysis follows a similar pattern to that appearing in Figure 3a. Thus, all of the potential impact sites are clustered near -40° latitude. The historical landing sites, marked in red in Figure 13, do not extend far into the Moon's southern hemisphere. Thus, an uncontrolled impact of KPLO will not risk disturbing these historical sites.

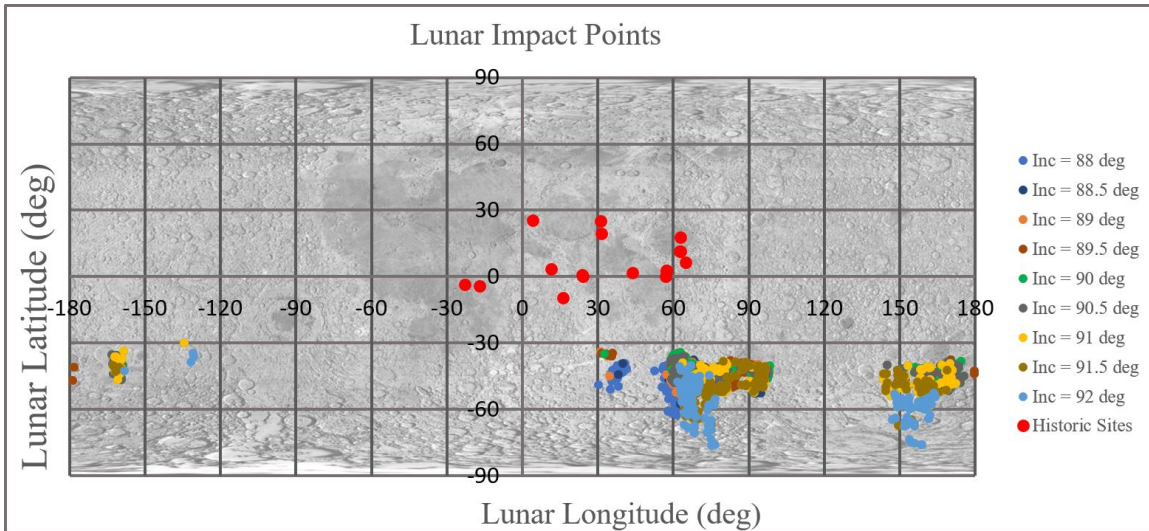


Figure 13. Potential KPLO impact sites and historic landing sites

SUMMARY AND CONCLUDING REMARKS

The KPLO spacecraft is scheduled to launch in late 2020 for insertion into a 100 km, circular, polar science orbit in 2021. A low cost, reliable stationkeeping method is proposed to maintain the spacecraft within altitude deadbands for a year-long science mission. Scheduled circularization control exploits patterns in the evolution of argument of perilune and eccentricity to schedule maneuvers that are small in magnitude, regularly scheduled, predictable in cost, and visible from Earth. The results are confirmed in Monte Carlo analysis. The SCC method saves significant Δv over a line-of-apsides control scheme similar to that used for operations of Lunar Prospector, Kaguya, and Lunar Reconnaissance Orbiter. However, the cost savings are achieved by allowing short excursions beyond a ± 30 km deadband every other month. Additionally, an assessment of spacecraft disposal by uncontrolled impact is performed, demonstrating that impacts occur in the southern hemisphere and do not threaten historical landing sites.

ACKNOWLEDGMENTS

The authors would like to thank Michael Mesarch and David Folta for their insight. Portions of this work were completed at NASA JSC under contract #NNJ13HA01C. Also, this work was supported by Korea Lunar Exploration Program funded by the Ministry of Science and ICT (MSIT, Korea)

REFERENCES

- ¹ Choi, S., R. Whitley, G. Condon, M. Loucks, J. Park, S.W. Choi, and S. Kwon, "Trajectory Design for the Korea Pathfinder Lunar Orbiter," AAS/AIAA Astrodynamics Specialists Conference, Snowbird, Utah, August 2018.
- ² Folta, D., K. Galal, and D. Lozier, "Lunar Prospector Frozen Orbit Mission Design," AIAA/AAS Astrodynamics Specialists Conference, Boston, Massachusetts, August 1998.
- ³ Lozier, D., K. Galal, D. Folta., and M. Beckman, "Lunar Prospector Mission Design and Trajectory Support," AAS/AIAA Spaceflight Mechanics Meeting, Monterey, California, February 1998.
- ⁴ Matsumoto, S., Ogawa, M., Kawakatsu, Y., Konishi, H., Ikeda, H., Terada, H., Tanaka, K., Kato, T., Otani, K., Kamikawa, E., Ikegami, S., "Flight Results of Selenological and Engineering Explorer "KAGUYA" on Lunar Orbit," 21th International Symposium on Space Flight Dynamics, Toulouse, France, September-October 2009.
- ⁵ Mesarch, M., M. Beckman, D. Folta, R. Lamb, and K. Richon, "Maneuver Operations Results from the Lunar Reconnaissance Orbiter Mission," SpaceOps 2010 Conference, Huntsville, Alabama, April 2010.
- ⁶ Beckman, M., "Mission Design for the Lunar Reconnaissance Orbiter," 29th Annual Guidance and Control Conference, Breckenridge, Colorado, February 2006.
- ⁷ Beckman, M. and R. Lamb, "Stationkeeping for the Lunar Reconnaissance Orbiter," 20th Annual International Symposium on Spaceflight Dynamics, Annapolis, Maryland, September 2007.
- ⁸ Folta, D. and D. Quinn, "Lunar Frozen Orbits," AIAA/AAS Astrodynamics Specialist Conference, Keystone, Colorado, 2006.